Contrib Mineral Petrol (1988) 100:246–260

Contributions to Mineralogy and Petrology

Grain growth in synthetic marbles with added mica and water

D.L. Olgaard* and B. Evans
Department of Earth, Atmospheric, and Planetary Sciences, Massachusetts Institute of Technology, Cambridge, MA 02139, USA

Abstract. Evolution of grain size in synthetic marbles was traced from compaction of unconsolidated powder, through primary recrystallization and normal grain growth, to a size stabilized by second phases. To form the marbles, reagent grade $CaCO_3$ was mixed with 0, 1 and 5 volume% mica and heat-treated under pressure with added water. Densification with negligible recrystallization occurred within one hour at 500° C and 500 MPa confining pressure. Primary recrystallization occurred at 500–550° C, causing increases of grain size of factors of 2–5. Resulting samples had uniform grain size, gently curved grain boundaries, and near-equilibrium triple junctions; they were used subsequently for normal grain growth studies. Normal grain growth occurred above 550° C; at 800° C, grain size (D) increased from 7 μm (D_0) to 65 μm in 24 hours. Growth rates fit the equation, $D^n - D_0^n = Kt$, where K is a constant and $n \simeq 2.6$. Minor amounts of pores or mica particles inhibit normal grain growth and lead to a stabilized grain size, D_{max}, which depends on the size of the second phases and the inverse of their volume fraction raised to a power between 0.3 and 1. Once D_{max} is reached, normal growth continues only if second phases are mobile or coarsen, or if new driving forces are introduced that cause unpinning of boundaries. Normal grain growth in Solnhofen limestone was significantly slower than in pure synthetic marble, suggesting that migration is also inhibited by second phases in the limestone.

Introduction

Grain size is an important microstructural parameter in rocks that affects physical and chemical properties. Some plastic flow mechanisms are grain-size sensitive, as are the kinetics of metamorphic and igneous reactions. Microstructure is also an important source of information about deformation events, e.g. textures of mylonites or fault breccias. Post-tectonic recrystallization may alter deformation-induced microstructures and textures, obscuring evidence for previous tectonic events and altering physical properties.

Ceramists and metallurgists have long recognized that grain boundary migration can be inhibited by precipitation or direct addition of discrete second phases (Kingery et al. 1976 Ch. 10). Both field and laboratory observations suggest that grain size of rocks may also be influenced by second phases and pores, which are ubiquitous (e.g. Hobbs et al. 1976 p. 112; Etheridge and Wilke 1979; Wilson 1979; and Evans et al. 1980).

In this study, we report experiments which trace the evolution of grain size from densification of calcite powder, through primary recrystallization and normal grain growth, ending with a grain size stabilized by second phases (Fig. 1). The objectives of the study were 1) to fabricate dense fine-grained single and two-phase synthetic marbles, and to characterize densification and recrystallization microstructures; 2) to measure grain size as a function of time, porosity, and mica content; and 3) to compare our results with those from similar experiments using natural calcite rocks. Our experiments showed that: 1) the kinetics of normal grain growth were affected by minor variations in porosity; 2) a stabilized grain size which depended on mica content

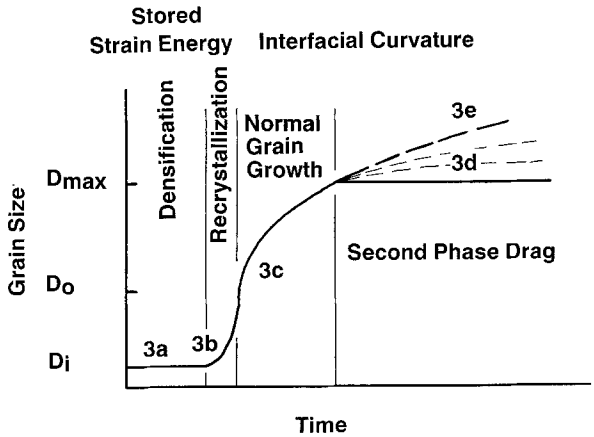

Fig. 1. Four regions of grain size evolution as observed in our experiments. D_i is the initial powder size; D_0 is the grain size at the beginning of normal grain growth, and D_{max} is the stabilized grain size. The removal of stored energy due to internal strains remaining from the densification stage drives primary recrystallization. Boundary migration during normal grain growth is driven by reduction in curvature of the interfaces. When the average grain size reaches the stabilized grain size, further boundary motion is retarded by drag forces owing to the second phase. If second phases are mobile, D_{max} may increase with time at rates less than those for normal grain growth. Approximate locations of the micrographs of Fig. 3a–e are indicated

* *Present address:* Geologisches Institut, Eidgenössische Technische Hochschule, CH-8092 Zürich, Switzerland

Offprint requests to: D.L. Olgaard

was reached in the calcite/mica polycrystals; and 3) normal grain growth in synthetic marbles was more rapid than in Solnhofen limestone at comparable temperatures. A study of normal grain growth in dry synthetic marbles is in progress.

Mechanisms and models

Densification

An uncompacted powder may densify by material transport from regions between grain centers to free surfaces. Densification may occur by combinations of dislocation flow, solution-transfer, and grain-boundary, lattice, or surface diffusion. With large applied pressure at 500–700° C, densification in calcite produces a microstructure with high residual dislocation density and tightly curved grain boundaries (see below). Caristan et al. (1981) have discussed densification mechanisms in both calcite and quartz polycrystals.

Primary recrystallization

During primary recrystallization, internal strain energy is reduced by the production and motion of grain boundaries (Kingery et al. 1976). Above a critical temperature, which is a function of strain energy, annealing time, heating rate, and initial grain size (Shewmon 1969 p. 94), strain-free grains form by migration of boundaries into regions with anomalously high dislocation densities, or by the progressive rotation of subgrains (Poirier and Guillopé 1979). When deformation accompanies recrystallization, the stable size which forms is called the dynamically recrystallized grain size and is a function of applied stress. In a matrix which has residual stored strain energy, but which is not deforming, new grains grow until they impinge on each other, and a strain-free matrix develops. This statically recrystallized grain size depends on the rates of nucleation and growth of new grains. In this paper, we discuss only primary or static recrystallization; for reviews of dynamic recrystallization, see Urai et al. 1986 and Drury et al. 1985.

Buerger (1930) first recognized that solid-state recrystallization was an important transformation process in geologic materials. The earliest experiments on compressed powders of anhydrite, fluorite and periclase (Buerger and Washken 1947), on several calcite rocks (Griggs et al. 1960) and on quartz (Hobbs 1968) showed that, in agreement with metals, a critical temperature for static recrystallization exists which depends on internal strain and interfacial energies, but which is relatively independent of annealing time.

Normal grain growth

The internal free energy of a polycrystal will be reduced as grain boundaries migrate toward their centers of curvature, reducing total grain boundary area (Fig. 2a). When recrystallization is driven by reduction of average grain boundary curvature, it is called normal grain growth. In two dimensions, a matrix of hexagonal grains of equal size may have straight grain boundaries. In three dimensions, however, no grain shape or size distribution exists which satisfies interfacial tension constraints at grain corners, which fills the space completely, and which has zero curvature. Therefore, grains will continue to grow until their boundaries are pinned by second phases or until the grain size is a small fraction of the sample size. Rarely is the latter case observed.

Normal grain growth has been studied in quartz and calcite contact aureoles (e.g. Joesten 1983; Keller et al. 1977; Robinson 1971; Spry 1969; Grigor'ev 1965; Edwards and Baker 1944; Covey-Crump and Rutter private comm.). Around these aureoles, grain size decreased with distance from the plutons, apparently correlating with estimated peak temperatures. In naturally recrystallized rocks containing second phases, the matrix grain size often varies inversely with second phase content (e.g. Hobbs et al. 1976; Etheridge and Wilke 1979; Christie and Ord 1980; Evans et al. 1980).

Experimental measurements of normal grain growth kinetics or stabilization of grain size by second phases in rocks are less common. Wilson (1979) found a qualitative inverse relationship between grain size and mica content in experimentally deformed polycrystalline ice. In contrast, Tullis and Yund (1982) concluded that minor amounts of second phases had little effect on normal grain growth in wet and dry quartzites and Solnhofen limestone.

The presence of water seems to influence normal grain growth in quartz and calcite. In Tullis and Yund's experiments, water significantly increased growth kinetics in quartzites, and, to a lesser extent, the limestone. Rutter (1983) observed significant normal grain growth ony above 800° C, and then only if water was present. He concluded that partial melting occurred. During deformation experiments with oven-dried Solnhofen limestone, Schmid et al. (1977) measured significant grain growth only at temperatures where voids filled with melt or ponded CO_2 formed.

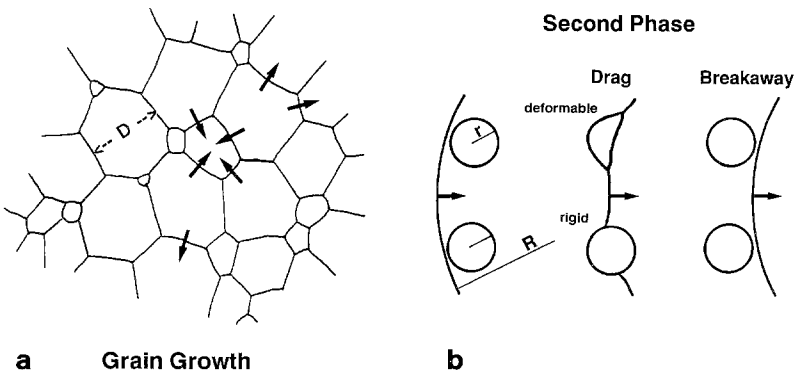

Fig. 2. a Normal grain growth occurs by migration of boundaries towards their centers of curvature. Small grains shrink and disappear, while large grains grow. The arrows indicate the direction of boundary migration; **b** When a migrating grain boundary with radius of curvature, *R*, encounters a second phase particle, continued migration is opposed by restraining forces proportional to the particle radius, *r*, and the number of second phases on the boundary. If the second phase particle is deformable, e.g. porosity, its effective radius may increase as the shape of the particle or pore responds to capillary forces

When large amounts of fluids are present and form a connected phase, as in experiments of coarsening of calcite powder in distilled water (Chai 1974), or of crystallization of quartz from a granitic melt (Jurewicz and Watson 1985), growth kinetics and size distribution follow Ostwald ripening models (Wagner 1961; Lifshitz and Slyozov 1961).

Kinetics of normal grain growth

Normal grain growth kinetics are often described by the equation:

$$D^n - D_0^n = Kt \quad (1)$$

where D and D_0 are the grain sizes at times t and $t_0 = 0$, respectively, K is a constant dependent on temperature and grain boundary mobility, and n is a constant dependent on the process controlling the growth rate. Theoretically, n equals 2 in a pure single-phase system (Burke and Turnbull 1952) and 3 in a system with pores or an interconnected fluid phase (Brook 1976; Lay 1968). Empirically, n is often found to be greater than 2; n may vary with time or temperature (Hu and Rath 1970).

In computer simulations of three-dimensional normal grain growth, Anderson et al. (1984) found n equal to 2.3–2.6 for a single-phase polycrystal with isotropic grain boundary energies. In contrast to the case of mobile pores, n was relatively unaffected by rigid second phases and minor anisotropy in grain boundary energy until growth was arrested by the second phases (Srolovitz et al. 1984 and Grest et al. 1985).

Grain size stabilized by second-phases

Boundaries cease migrating when the restraining pressure of any second phases equals the driving pressure for migration (Zener 1948; Fig. 2b). If the second phase particles are also rigid and immobile, the grain size is fixed. If the second phases are mobile, boundaries may drag them, possibly causing them to coalesce (Ashby and Centamore 1968). In either case, the grain size is controlled by the instantaneous size, volume fraction, and geometry of dispersion of the second phase.

The effect of second phases on the stable matrix grain size is given by the equation:

$$D_{max} = C(d/f^m) \quad (2)$$

D_{max} is the stable, matrix grain-diameter; d is the second phase diameter; f is the second phase volume fraction; C is a constant; and m is a constant dependent upon the second phase dispersion parameters (see Zener 1948; Gladman 1966; Haroun and Budworth 1968; Hellman and Hillert 1975; Anand and Gurland 1975; Louat 1983; Nes et al. 1985; and Olgaard and Evans 1986 for reviews). For second phases dispersed randomly throughout the matrix, along grain boundaries, or only at grain corners, m equals 1, 1/2, or 1/3, respectively.

It is difficult and tedious to measure directly the dispersion of second phases within a polycrystal, but one obtains an indirect characterization using (2) and measurements of D_{max}, d and f. Olgaard and Evans (1986) determined that m varied from 0.3 to 0.6 for Al_2O_3 particles in a calcite matrix and from 0.2 to 1.0 for a variety of metals and ceramics with both mobile and immobile second phases. These results indicate a preference for second phases to concentrate at grain boundaries or corners.

Experimental method

The experiments involved four steps: 1) initial characterization and mixing of the powders, 2) fabrication of dense, fine-grained synthetic marbles, 3) heat-treatment of the marbles to induce primary recrystallization and normal grain growth, and 4) grain size measurements and microstructural characterization.

In the initial preparation step, reagent grade $CaCO_3$ powder was mechanically mixed in ethanol for four hours with 0, 1, or 5 volume% of finely ground biotite or phlogopite. The powders were sized by X-ray sedimentation, single-point N_2 adsorption (BET) (Allen 1981 pp. 285, 465), and optical and transmission electron microscopy (TEM) (Table 1).

The powder mixtures were then densified and recrystallized by a series of cold and hot isostatic presses. Two cold presses at 150 MPa produced a friable aggregate which was approximately 80% dense. In the early experiments (1007–4003, Tables 2–3), samples were heat-treated at 700–900($\pm$10)° C, for up to 24 h in an internally heated pressure vessel using argon as the confining medium (Olgaard and Evans 1986). The confining pressure (P_c) and $H_2O + CO_2$ pore pressure (P_p) conditions were either $P_c = 300 \pm 5$ MPa and $P_p = 2 \pm 1$ MPa, or $P_c = 400$ MPa and $P_p = 100$ MPa (i.e., $P_c - P_p = 300$ MPa) For brevity, this group of experiments is referred to as "XOXX".

As discussed below, porosity appeared to have a major effect on the kinetics of normal grain growth. Therefore, in later experiments (CA-1 to CA-19, referred to as "CA–XX"), a one hour, fabrication step with $P_c = 500$ MPa, $P_p = 2$ MPa, $T = 550$–650° C was added to produce high density, recrystallized starting materials with more uniform porosity. During this fabrication, the pore pressure was allowed to equilibrate for one-half hour or more after the last cold press. Heating and cooling rates were 40° C/min and 80° C/min, respectively.

Table 1. Mica and $CaCO_3$ powder diameters (μm)

Method	$CaCO_3$	Biotite	Phlogopite
Optical microscopy	4.9 ±4	5 ±3.5	2.5 ±2 4.0 ±3
TEM			
Max			1.3 ±0.5
Min			0.4 ±0.2
Int			0.39
BET			
Before	3.2		0.15, 0.26
After	0.80		
X-ray sedimentation			
50 mass %	5.8		4.2
50 vol. %	0.65		0.0023 (?)

Optical microscopy: Average diameter of particles intersecting a test line

TEM: Diameters of plate-like particles measured from micrographs. Average *max*imum and *min*imum diameters of particles on grain boundaries and average diameter of particles in grain *int*eriors

BET: Equivalent spherical diameter calculated from surface area measured by single-point N_2 absorption *before* and *after* grinding and mixing

X-ray sedimentation: Equivalent spherical diameter at 50 mass percent (directly from the data) and at 50 volume percent (after Herdan 1960). For the shape of the size distributions see Olgaard (1985)

(?) Impossibly small. Method not directly applicable to these particles

Table 2. Grain growth data for pure $CaCO_3$

Run #	Temp. (° C)	P_c/P_p (MPa) 400/100	P_c/P_p (MPa) 300/2	Time[b] (10^3 s)	Rate[c]	D (μm)	Porosity (%)	Met.[d]	Pore size[e] (μm)
CA-19	500	(500/2)		3.6		5.1[f]			
CA-10	550	(500/2)		3.6		10.7			
CA-2	650	(500/2)		3.6		13.3			
CA-3	650	(500/2)		3.6		23.0			
CA-4	650	(500/2)		3.6		10.5			
2056	700		x	0.6		10.0			
2055	700		x	0.6		7.0			
2052	700		x	3.6		8.7	5.7	IM	
2042	700		x	7.2		12.6			
2043	700		x	7.2		11.9			
2045	700		x	7.2		11.7			
2053	700		x	27.0		15.0			
2024	800	x		0.01	0	12.8	10.3	OPT	1.7 I 4.3±3.8 E
2034	800		x	0.01	+	12.9			
2039	800	x		0.01	−	7.6			
2049	800		x	0.3	0	10.7			
1009	800	x		2.1	−	12.3	5.5	IM	
2006	800	x		3.6	0	17.7	1.9	IM	
CA-13[a]	800		x	3.6		20.9			
2020	800	x		3.8	0	23.5			
1008	800	x		7.2	−	18.8	6.3	IM	
								OPT	3.1±2 T
2033	800		x	7.2	0	31.4			
2037	800	x		7.2	−	20.6			
2042	800	x		7.2	0	25.4			
2045	800		x	7.2	+	39.6			
4003	800		x	7.2	0	23.1			
2021	800	x		7.3	+	35.0	2.7±0.5	OPT	1.4±0.5 I 3.5±2.0 E
							5.0	SEM	
2022	800	x		9.3	0	33.1	3.2±0.6	OPT	
1007	800	x		10.8	0	36.0			2.9±1.4 I
2026	800	x		10.8	−	26.4	8 ±1	OPT	
2023	800	x		12.6	+	48.0	3.8	OPT	
							5	SEM	
2004	800	x		14.4	−	15.0	3	IM	
2028	800	x		14.4	−	23.0			
2025	800	x		16.6	−	25.2	8.3	OPT	
2005	800	x		20.5	0	40.2	2.3	IM	
2053	800		x	27.0	−	23.8			
2048	800		x	36.0	−	24.5			
2054	800		x	36.0	0	42.9			
CA-12[a]	800		x	36.0		63.1			
2007	800	x		38.0	−	23.3	3.5±0.8	IM	
2047	800		x	86.4	−	44.3			
CA-11[a]	800		x	86.4		68.8			
CA-15[a]	800		x	86.4		65.9			
2027	900	x		3.6		36.3			
CA-18[g]	900		x	36.0		62.7			

[a] Initially isostatically hot pressed in CA-2, 3, 4, or 10
[b] Elapsed time at temperature
[c] At 800° C, the rate of grain growth in the XOXX experiments was faster than (+), slower than (−), or equal to (0) the rate in the CA−XX experiments
[d] Method of porosity measurement; OPTical microscope, Scanning Electron Microscope, IMmersion in CCl_4
[e] Pore size measured from optical micrographs. Interior, Edge, and Total pores
[f] Unrecrystallized. D probably overestimated because of difficulty in measuring very small grains
[g] Purposely fabricated with a high porosity for the melt determination test

Table 3. Grain growth data for $CaCO_3$/mica and Solnhofen limestone

Run #	Temp. (°C)	P_c/P_p (MPa) 400/100	P_c/P_p (MPa) 300/2	Time[b] (10^3 s)	Mica[c]	D (μm)	Porosity (%)	Met.[d]	Pore size[e] (μm)
1% mica									
2039	800	x		0.01	p	9.9			
2049	800		x	0.3	p	7.2			
2002	800	x		0.5	b	6.5			
2006	800	x		3.6	b	15.7	0.0	IM	
2003	800	x		7.2	b	13.2			
2037	800	x		7.2	p	15.8			
2004	800	x		14.4	b	13.9	3	IM	
2005	800	x		20.5	b	32.3	1.2	IM	
2053	800		x	27.0	p	21.3			
2007	800	x		38.0	b	26.4	2.0	IM	
5% mica									
CA-9	650	(500/2)		3.6	p	9.2			
2024	800	x		0.01	p	12.2	10 ±1	OPT	2.5±1.1 E
2034	800		x	0.01	p	8.7			
2039	800	x		0.01	p	7.6			
2049	800		x	0.3	p	6.3			
2006	800	x		3.6	b	11.4	1.7	IM	
CA-13[a]	800		x	3.6	p	12.0			
2020	800	x		3.8	p	15.6			
2033	800		x	7.2	p	13.7			
2037	800	x		7.2	p	10.5			
2021	800	x		7.3	p	23.1	15.5±1.0	OPT	1.0±0.6 I 3.0±1.5 E
2022	800	x		9.3	p	22.2	15 ±2	OPT	
2026	800	x		10.8	p	19.2			
2023	800	x		12.6	p	23.9	11.3±1	OPT	
2028	800	x		14.4	p	14.4			
2025	800	x		16.6	p	17.3	8.3±0.9	OPT	1.1±0.6 I 2.4±0.8 E
2005	800	x		20.5	b	17.6	2.2	IM	
2053	800		x	27.0	p	12.0			
2048	800		x	36.0	p	16.3			
CA-12[a]	800		x	36.0	p	13.6			
2007	800	x		38.0	b	15.8	1.4	IM	
2047	800		x	86.4	p	17.5			
CA-11[a]	800		x	86.4	p	16.9			
CA-15[a]	800		x	86.4	p	17.4			
Solnhofen limestone									
Initial						6.2			
0007	700		0.1 (CO_2)	8.4		6.3			
0009	700		0.1 (CO_2)	86.4		6.1			
0011	700		0.1 (CO_2)	95.4		6.2			
0013	700		0.1 (CO_2)	349.0		6.4			
0015	700		0.1 (CO_2)	432.0		6.6			
4133	800	x		0.3		6.3			
4137	800	x		2.3		6.6			
4130	800	x		15.2		7.6			
2054	800		x	36.0		11.0			
CA-18	900		x	36.0		17.1			

[a] Initially isostatically hot pressed in CA-9
[b] Elapsed time at temperature
[c] phlogopite/biotite as second-phase particles
[d] Method of porosity measurement; OPTical microscope, Scanning Electron Microscope, IMmersion in CCl_4
[e] Pore size measured from optical micrographs. Interior, Edge, and Total pores

Some experiments were done with both lithographic and massive samples of Solnhofen limestone cored perpendicular to the fabric; these had an initial grain size of 6.1 μm. The 700° C specimens were run at 0.1 MPa in CO_2. The 800 and 900° C samples were placed in the sample column with the synthetic specimens without any other special treatment.

The matrix grain size was measured with a transmission optical microscope in ultra-thin sections (5–10 μm thick) using the linear intercept method. Following Exner (1972), the average grain diameter (D) was expressed as 3/2 the mean linear intercept length, a conversion appropriate for equi-sized spheres (Underwood 1970). For more realistic shapes, the conversion factor differs only by a small constant factor.

The mechanisms (and therefore the kinetics) of normal grain growth are altered by the presence of a liquid phase along the boundary (Greenwood 1956; Lay 1968; Yan et al. 1977). Darkfield TEM imaging was used to detect the presence and distribution of amorphous or very fine-grained material (Olgaard and Evans 1986). TEM and SEM were also used to examine the distribution of the particles and pores between the matrix and the grain boundaries and to detect particle agglomeration.

Results

Densification and primary recrystallization

Cold-pressed aggregates with initial relative density of 0.8 (i.e. $0.8 \times$ the density of a single crystal) transformed to nearly dense marbles with unconnected porosity and polygonal grains when isostatically hot-pressed above 550° C with $P_c = 500$ MPa and $P_P = 2$ MPa (Fig. 3c). The maximum relative densities of samples heated with water were 0.95–0.98 (Table 2, immersion method). Samples densified after being oven-dried in air, had densities up to 0.99 (Caristan et al. 1981; Olgaard 1985). The pemeability of similar synthetic marbles dropped nearly to zero ($k \simeq 1$ nanodarcy or 10^{-21} m^2) at approximately 0.95 relative density (Bernabé et al. 1982) indicating that the final porosity was unconnected. Two- to five-fold increases in grain size occurred after densification and during primary recrystallization. Although it was difficult to distinguish between the end of primary recrystallization and the onset of normal grain growth, based on microstructures, we concluded that the completion of primary recrystallization occurred in less than one hour at 500–550° C. Mica particles had no obvious effect on densification or primary recrystallization.

Microscopic observations

The progressive development of microstructures during recrystallization and grain growth was investigated with optical microscopy, SEM, and TEM (Figs. 3–5). The latter stages of primary recrystallization and the onset of grain growth are characterized by fine, relatively strain-free grains (Fig. 3c). After short heat-treatments at 800° C, polygonal grains with near-equilibrium triple junctions (120° angles in plane section) developed.

In samples with the minimum porosity, grain size increased five-fold in 2–4 h at 800° C (Fig. 3e). With higher porosity or with mica particles, the grain size achieved in a given time was smaller (Fig. 3d). Intergranular pores were lens-shaped on grain edges and equant at triple junctions (Fig. 4a–b). Intragranular pores were often polygonal in shape, clustered in the centers of grains, and smaller than the intergranular pores. Plate-shaped mica particles were a) dispersed along grain boundaries with their shortest dimension normal to the boundary plane (Fig. 4c); (b) clustered in fluid phases at triple junctions (Fig. 4d); or c) dispersed in grain interiors. Grain boundaries which contained pores and particles, were often bowed, suggesting that second phases imposed a drag force on the migrating boundaries.

Most dislocations in the heat-treated samples were non-interacting, straight and parallel, or gently curved and loosely tangled; subgrain boundaries were rare (Fig. 4e). Many of the dislocations, open or cracked grain boundaries and twins may have resulted from high thermal stresses developed during the sample quench; calcite has one of the largest thermal expansion anisotropies of any mineral (Rosenholtz and Smith 1949; Skinner 1966).

Wet specimens heated over 700° C contained an intergranular film of amorphous or cryptocrystalline material which probably resulted from partial melting (Olgaard and Evans 1986). Such a film may have influenced the boundary migration mechanism by coating the mica particles, thereby mobilizing them into the clusters observed at triple junctions (Fig. 4d) (cf. Ashby and Centamore 1968).

Excepting a few, very large grains (> 30 μm) (Fig. 5a), the initial microstructure of the Solnhofen limestone is similar to that of unrecrystallized synthetic marble (compare Figs. 3b and 5a). When measurable grain growth occurred in Solnhofen limestone, the optical microstructure resembled that of the synthetic marbles of comparable grain sizes (Fig. 5b). Other optical and TEM microgrphs of Solnhofen limestone are shown by Griggs et al. (1960), Barber and Wenk (1973, 1979), Schmid et al. (1977) and Tullis and Yund (1982).

Kinetics of normal grain growth

Normal grain growth data for synthetic marbles with water added are listed in Table 2 and plotted in Fig. 6. Each data point is the average grain diameter, D, for all measurements on a single sample; the bars represent the measured spatial inhomogeneity in D. Standard deviations of D for both coarse- and fine-grained samples were approximately ± 12 percent. The uncertainties resulting from observer bias and preferred orientation were estimated to be ± 2 percent. A linear regression of the CA−XX data at 800° C to (1) (solid line) gave n equal to 2.6 ± 0.1; at 700 and 900° C (XOXX series), n was 3 or greater. CA-18 (900° C) was designed to produce substantial melt, and, therefore, had an anomalously high porosity and anomalously small grain size.

In agreement with Rutter (1983), no grain growth occurred in our 700° C Solnhofen limestone experiments (Table 2, Fig. 7). These samples showed slight microstructural alteration only at the longest times. At 800° C, the matrix recrystallized in all cases; however, normal grain growth was measurable only for times over 4 h. At 900° C, normal grain growth was more noticeable, but still less than the minimum measured in the synthetic marbles at 800° C.

Inhibition of normal grain growth by mica particles and pores

Calcite grain growth was suppressed by dispersed mica particles in volume fractions of 1 and 5 percent in less than 6 h (Fig. 8). Grain growth was arrested within 6 and 2.5 h for samples with 1 and 5 vol% mica, respectively; D_{max} was 28 and 17 μm, respectively. In Fig. 9, the effects of mica on D_{max} are compared with data from Olgaard and Evans (1986) and with (2) setting C equal to 1 and m equal

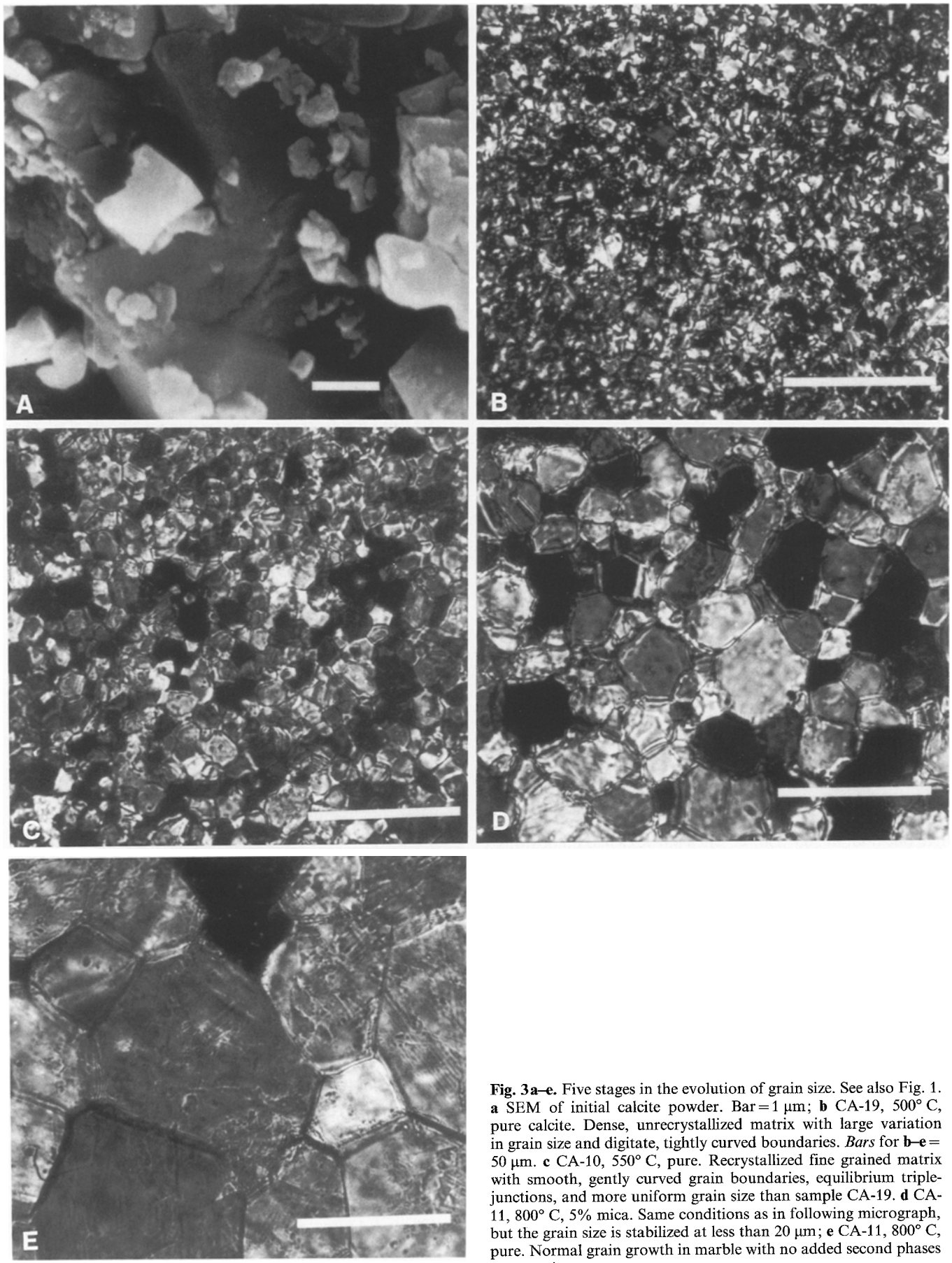

Fig. 3a–e. Five stages in the evolution of grain size. See also Fig. 1. **a** SEM of initial calcite powder. Bar = 1 μm; **b** CA-19, 500° C, pure calcite. Dense, unrecrystallized matrix with large variation in grain size and digitate, tightly curved boundaries. *Bars* for **b–e** = 50 μm. **c** CA-10, 550° C, pure. Recrystallized fine grained matrix with smooth, gently curved grain boundaries, equilibrium triple-junctions, and more uniform grain size than sample CA-19. **d** CA-11, 800° C, 5% mica. Same conditions as in following micrograph, but the grain size is stabilized at less than 20 μm; **e** CA-11, 800° C, pure. Normal grain growth in marble with no added second phases

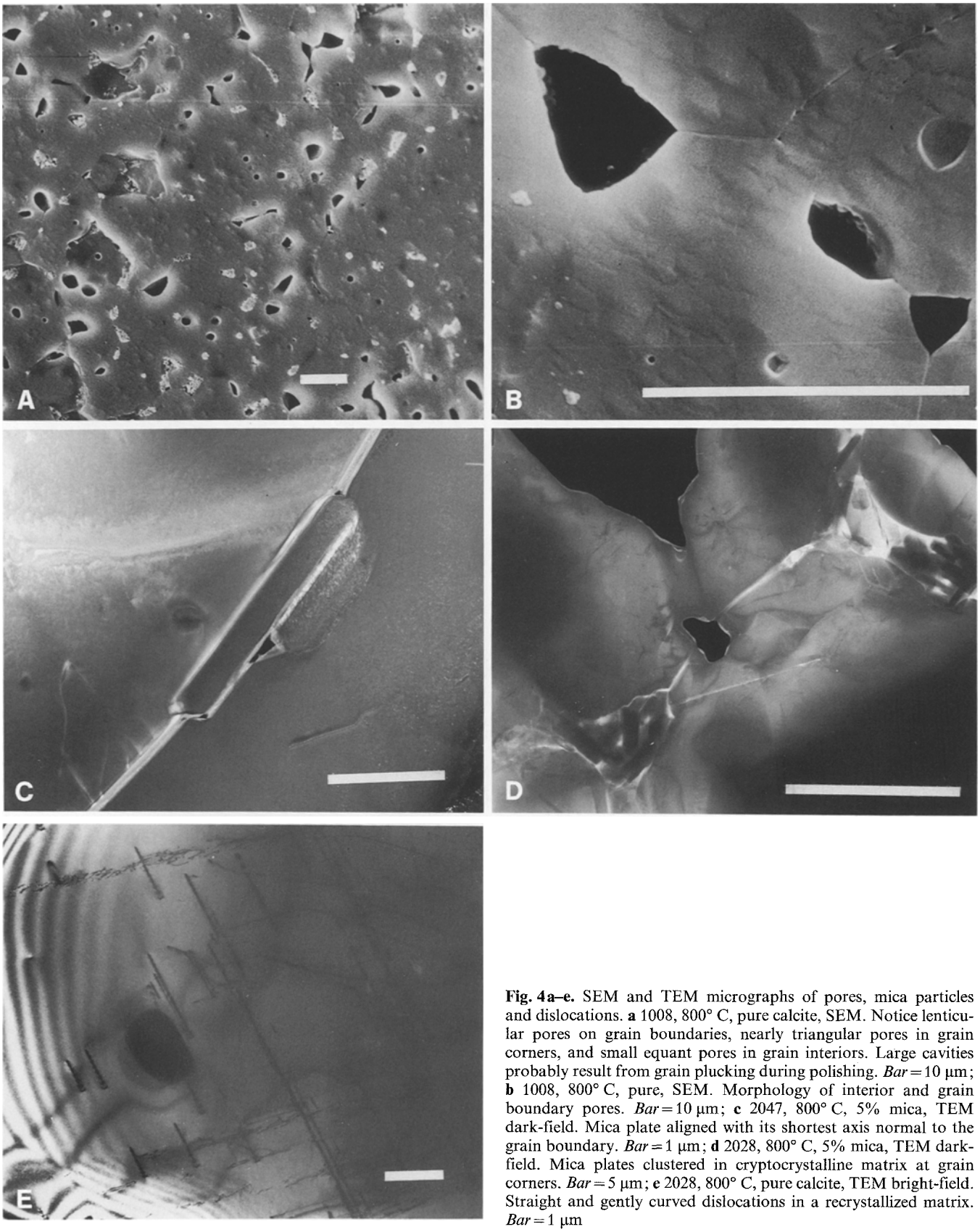

Fig. 4a–e. SEM and TEM micrographs of pores, mica particles and dislocations. **a** 1008, 800° C, pure calcite, SEM. Notice lenticular pores on grain boundaries, nearly triangular pores in grain corners, and small equant pores in grain interiors. Large cavities probably result from grain plucking during polishing. *Bar* = 10 μm; **b** 1008, 800° C, pure, SEM. Morphology of interior and grain boundary pores. *Bar* = 10 μm; **c** 2047, 800° C, 5% mica, TEM dark-field. Mica plate aligned with its shortest axis normal to the grain boundary. *Bar* = 1 μm; **d** 2028, 800° C, 5% mica, TEM dark-field. Mica plates clustered in cryptocrystalline matrix at grain corners. *Bar* = 5 μm; **e** 2028, 800° C, pure calcite, TEM bright-field. Straight and gently curved dislocations in a recrystallized matrix. *Bar* = 1 μm

to 1, 1/2, and 1/3. The maximum plate diameter, d_{TEM} = 1.3 μm, was used. If (2) is fit to the data by least squares, m is found to be 0.29, consistent with the $CaCO_3/Al_2O_3$ data.

Variations in porosity were probably the major cause of the variations in normal grain growth kinetics (Figs. 6 and 8). Minor chemical impurities and dislocation densities introduced during the preparation may also be important.

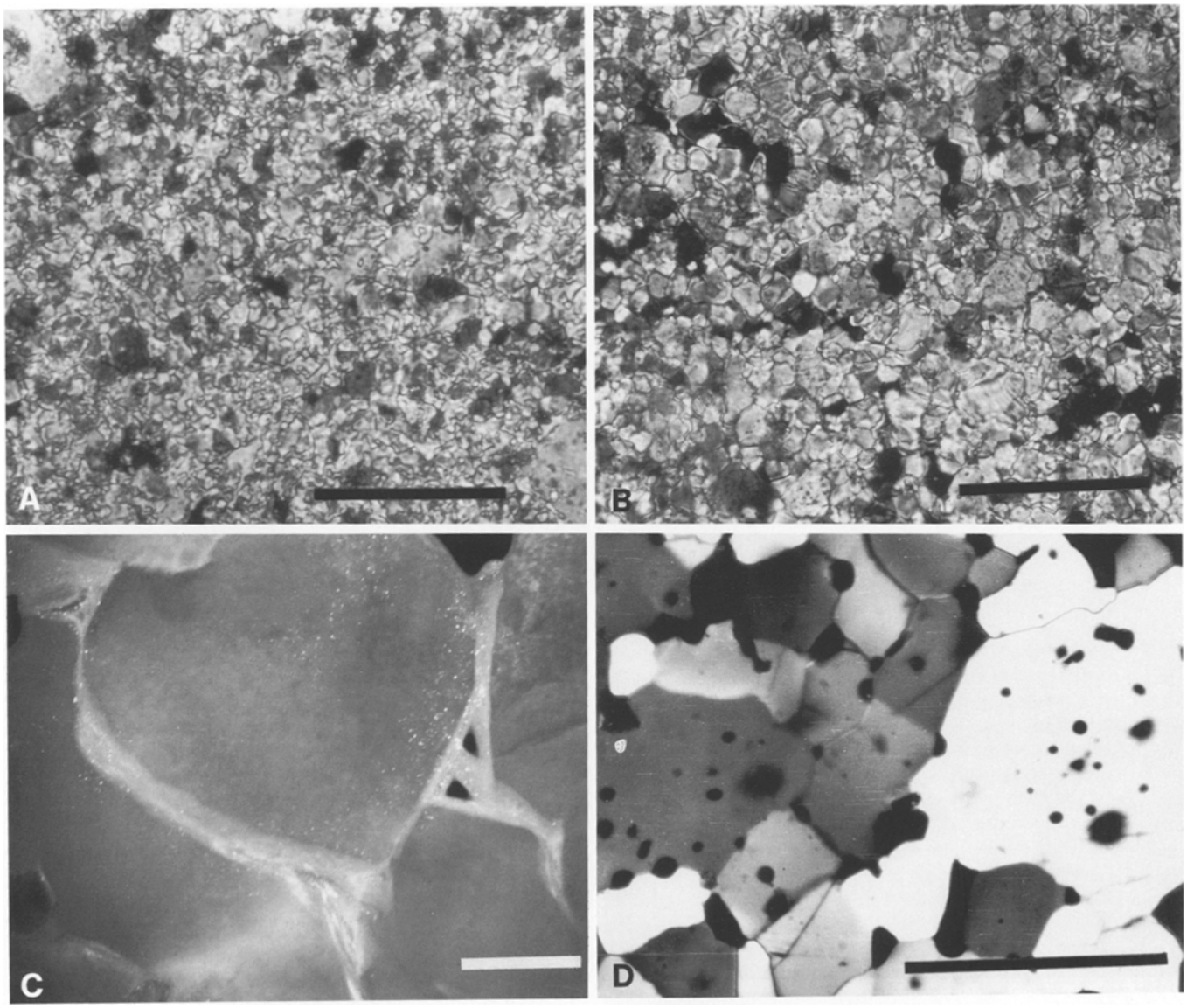

Fig. 5a–d. Solnhofen limestone. **a** Initial microstructure. Bar = 50 μm; **b** 2054, 800° C. Microstructure similar to that in recrystallized synthetic marbles of similar grain size (Compare to Fig. 3c). *Bar* = 50 μm; **c** TEM dark-field, initial. A phase of unknown composition lies along the grain boundary. *Bar* = 0.5 μm **d** 1000° C, P_c = 300 MPa, 4 h, oven dry. Significant normal grain growth has occurred; the large pores may contain material which melted during the experiment. *Bar* = 50 μm. (Courtesy S. Schmid)

Porosities were measured by three methods: weight loss of samples during immersion in CCl_4 (IM), and point counting using optical (OPT) and scanning electron (SEM) microscopes. IM probably reflects the minimum value because only the unconnected porosity is measured. Because coarse-grained samples disaggregated, IM could not be used when D was greater than 25 μm. OPT and SEM are probably overestimates. For OPT, the thickness of the thin section was difficult to estimate, and for both OPT and SEM, grain plucking during specimen preparation could not be avoided. For the samples containing mica, OPT also counted a substantial number of the mica particles as pores and, therefore, may reflect the total second phase content.

For pure calcite samples, there is a qualitative correlation between porosity and grain size (Table 2). Grain size in XOXX specimens with porosities greater than 4–6% were less than those in the CA−XX specimens. For calcite/mica samples, there is no obvious correlation between D and porosity because mica also influences the stabilized grain size. In all cases where the size of pores were measured, those on grain edges were larger than those in grain interiors.

Discussion

Densification and primary recrystallization

In order to measure normal grain growth, it is desirable to produce nearly dense samples with low dislocation densities: Pores inhibit boundary migration during grain growth. Internal strain energy – the reduction of which is the driving force for static recrystallization – is typically an order of magnitude or more larger than interfacial energies – the source of driving force for normal grain growth (Ashby 1980).

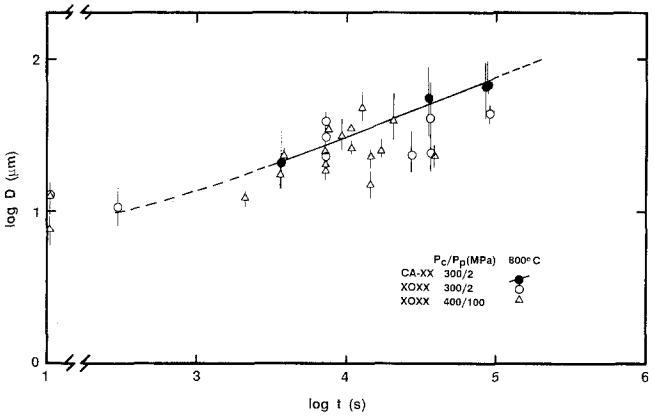

Fig. 6. Normal grain growth in synthetic marbles at 800° C. *Solid line* is a linear regression of Eq. (1) through the CA−XX data for $n=2.6$. Variatons in D for XOXX are presumably due to porosity

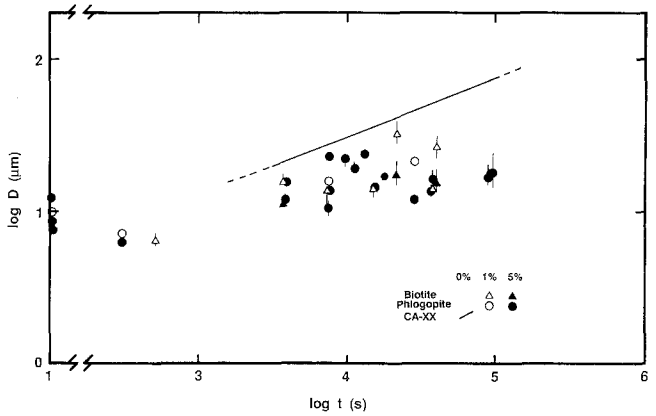

Fig. 8. Normal grain growth data for synthetic marble containing biotite or phlogopite as a second phase. Solid line for CA−XX data at 800° C is included for comparison. A stabilized grain size was reached in specimens with either 1 or 5 vol% mica in less than 5 h. No difference was detected in the stabilized grain size for samples with similar amounts of phlogopite or biotite

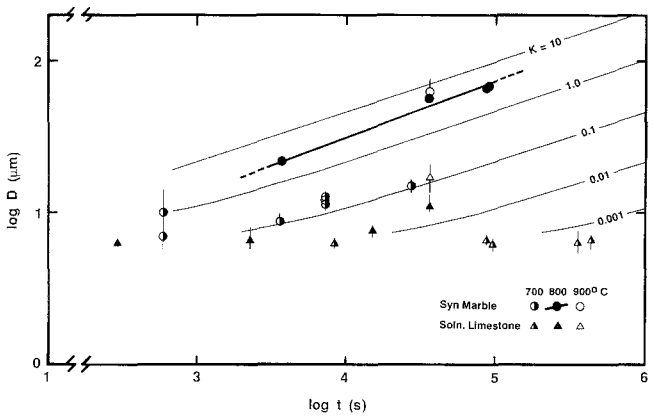

Fig. 7. Normal grain growth in synthetic marble and Solnhofen limestone at 700–900° C. Diagram has been contoured in orders of magnitude of K (Eq. 1) assuming $n=3$. For 800° C, only the CA−XX data, i.e. samples with the least porosity, are included

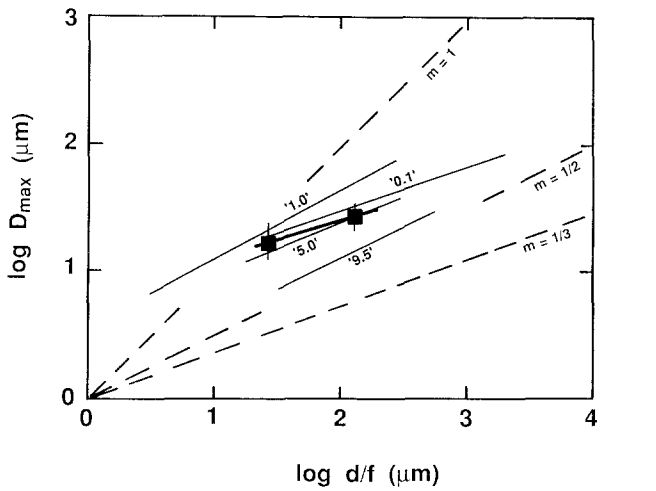

Fig. 9. Log of stabilized grain size, D_{max}, versus log of the second phase parameter, d/f. Solid squares and the heavy line are for marbles containing mica, $d_{mica}=d_{TEM}=1.3$ μm. The light lines are for data from Olgaard and Evans (1986) for marbles containing Al_2O_3. Each line is fit to experiments with constant d; slopes give the volume fraction exponent m in Eq. 2. The numbers, e.g. '0.1', refer to the nominal grit sizes of the Al_2O_3 particles in μm. Dashed lines are shown for $m=1$, 1/2, and 1/3, assuming $C=1$

In these experiments, suitable samples were fabricated from powders in a short time by utilizing high confining pressures and moderate temperatures, although neither porosity nor internal strain were ever completely eliminated. Apparently, the high confining (lithostatic) pressure induced plastic deformation at grain-grain contacts and promoted rapid porosity reduction. Moderate temperatures also promoted plastic deformation and, except for an initial period, did not cause boundaries to break away from the pores. Experience with sintering of commercial ceramics shows that porosity which remains attached to a boundary may be more easily removed than porosity included within a grain (Kingery et al. 1976).

In all experiments, including those at temperatures as low as 550° C, there was a rapid initial increase of grain size (cf. Fig. 3b and c). The resulting matrix had low dislocation density, relatively smooth grain boundaries, and equant grains, sometimes with included porosity. In the first few minutes after densification, boundary mobilities may become large enough to overcome the retarding forces caused by insoluble second phases and porosity, resulting in their inclusion in the recrystallizing grain (Rossi and Burke 1973). Static recrystallization experiments done on natural calcite aggregates strained to 10% or more indicate that recrystallization occurs above 500° C (Griggs et al. 1960). Thus, we believe that the initial rapid increase in grain size resulted from static recrystallization driven by reduction of the internal energy stored as dislocations and digitate boundaries.

It is possible to estimate the point at which normal grain growth becomes the dominant microstructural transformation process. The driving pressure for normal grain growth (P_{gg}) is given by:

$$P_{gg}=2\gamma/R \tag{3}$$

where γ is the interfacial energy per unit area (Zener in Smith 1948). The boundary radius of curvature, R, equals

αD where α is a constant of order 1–10 for gently curved boundaries (Smith 1948; Haroun and Budworth 1968).

Stored dislocation density, ρ, results in a driving pressure, P_ρ given by:

$$P_\rho = (1/2)\mu b^2 \rho \quad (4)$$

(e.g. Takeuchi and Argon 1976), where μ is the elastic shear modulus and b is the average Burgers vector. Setting (3) equal to (4), the dislocation density that would contribute a driving pressure equal to the curvature forces may be calculated. For calcite, approximate values of γ, μ, and b are 0.1 J/m^2, 25 GPa, and 0.63 nm, respectively (Janczuk et al. 1983; Hay 1987; Goetze and Kohlstedt 1977). With D_0 equal to 7 μm, and $\alpha = 1$, this dislocation density is 6×10^{12} m^{-2} (6×10^8 cm^{-2}).

The dislocation density in an unrecrystallized specimen, CA-19, was estimated to be 2×10^{13} m^{-2}, implying that the internal strain energy was high enough to drive recrystallization. In two samples heat-treated at 800° C, dislocation densities were estimated to be 10^{11} m^{-2} (less than one percent of that present before recrystallization). These few dislocations may have remained from the initial densification, or may have been introduced by thermal expansion stresses arising during quench. Following Wong and Brace (1979) and Rosenholtz and Smith (1949), a temperature change of 800° C in calcite may produce internal stresses greater than 1 GPa. Thus, we suppose that above 500° C, the initial rapid increase in grain size is due to primary recrystallization, followed by a longer period of normal grain growth.

Kinetics of normal grain growth

The grain size exponent, n, of (1) depends on the rate-limiting step for boundary migration. Theoretically, n may vary from 2 to 4 depending on the process (Nielsen 1966; Nichols 1966; Brook 1976). For many metals, n decreases with increasing temperature from 5 or more to 2 at the melting point (Hu and Rath 1970). In other cases, n is relatively constant, but always greater than 2; only in the highest purity metals does n equal 2. Linear regression of (1) through the 800° C, CA−XX data gives a value of 2.6 ± 0.1 for n, although n may increase with decreasing temperature and, possibly, with increasing time. For migration limited by pore drag or by motion of a liquid film, n is expected to be 3 (Lay 1968; Brook 1976).

Several microstructural observations also suggest that normal grain growth was controlled by pores or a boundary film: 1) Pores attached to the grain boundaries were distorted, suggesting pore drag (Hsueh et al. 1982). 2) Pores at grain corners and edges were larger than those in grain interiors (Table 2), indicating pore coarsening and coalescence along the boundaries (Kingery and Francois 1965). 3) Average grain sizes were smaller in regions of high porosity than low, implying that grain growth was restricted by the pores. 4) Thin intergranular films were observed along many boundaries in samples heat-treated at 700° C or more (Olgaard and Evans 1986).

In common with some metals, the rate of normal grain growth in the synthetic marbles appears to decrease with time during isothermal experiments (Figs. 6 and 8). (Decreasing growth rates are manifested as apparent decreases in K or increases in n with time.) Decreasing growth rates can be explained in at least two ways. First, there may have been variations in D_0 resulting from slight differences in preparation. We have chosen D_0 from the grain sizes of the shortest, lowest temperature experiments in which primary recrystallization occurred. For these experiments, D_0 ranged from a minimum of 7 μm to 10 μm or more. When the final grain size is 15 μm, this variation in D_0 gives uncertainties in K of at least 20%. Secondly, for longer times, moving boundaries capture mobile second phases, especially pores, that were in grain interiors, thereby increasing the drag force on the boundary and decreasing the growth rate.

Pores clearly have a major effect on the kinetics of normal grain growth. Although it was difficult to eliminate porosity completely, an intermediate, high-pressure fabrication step significantly reduced the variability in porosity: the CA−XX data fit equation 1 more consistently and, in most cases, have higher K than the XOXX data.

Liquid films along grain boundaries also effect normal grain growth. Yan et al. (1977) present mobility data for several oxides and show that a grain-boundary film increases mobility in those systems containing even a small amount of porosity. Bennison and Harmer (1985) showed that in exceptionally clean, dense Al_2O_3, a liquid phase reduced K. We conclude that, although grain-boundary films may accelerate kinetics when second phases are present, exceptionally clean synthetic marbles should have normal grain growth rates which are even faster than two-phase marble with fluid-films. Preliminary, unpublished results from normal grain growth in relatively pure, dense, dry synthetic marbles indicate that the growth rates are indeed an order of magnitude faster than those in wet marble at similar temperatures.

Thermal activation

To predict normal grain growth at lower temperatures requires knowledge of the activation energy for the process. The kinetics constant, K, usually follows an Arrhenius relation of the form:

$$K = K_0 exp(-Q_{gg}/RT) \quad (5)$$

where Q_{gg} is the activation energy, T is temperature, and K_0 and R are constants. Q_{gg} is similar to that for grain boundary diffusion, and sometimes is about half that for lattice diffusion (Kingery et al. 1976). Kronenberg et al. (1984) and Anderson (1969) measured activation energies of 360 ± 60 KJ/mole for lattice diffusion of carbon and oxygen in calcite between 500 and 800° C. Preliminary estimates from our data assuming $n = 3$ give Q_{gg} of 150 ± 80 KJ/mole. However, this value must be used with caution, because n is not necessarily constant, and because the range of temperature is very small.

Grain sizes in natural marbles are commonly ~100 μm to several millimeters. Assuming the kinetics follow (1) and (5) with $n = 3$, $Q_{gg} = 150$ KJ/mole, and K (800° C) = 4 μm^3/s, an increase in D from 5 μm to 100 μm or 1 mm at 300° C (~10 km depth) would take 10^4 and 10^7 years, respectively. (Although such times are relatively rapid for many metamorphic events, minor changes in Q_{gg} or temperature would change the calculated times significantly.) Assuming (2) is applicable to normal grain growth in the earth, with second phase particles of 5 μm, and if $m = 0.4$, normal grain growth would be stabilized at 100 μm and 1 mm for second phase

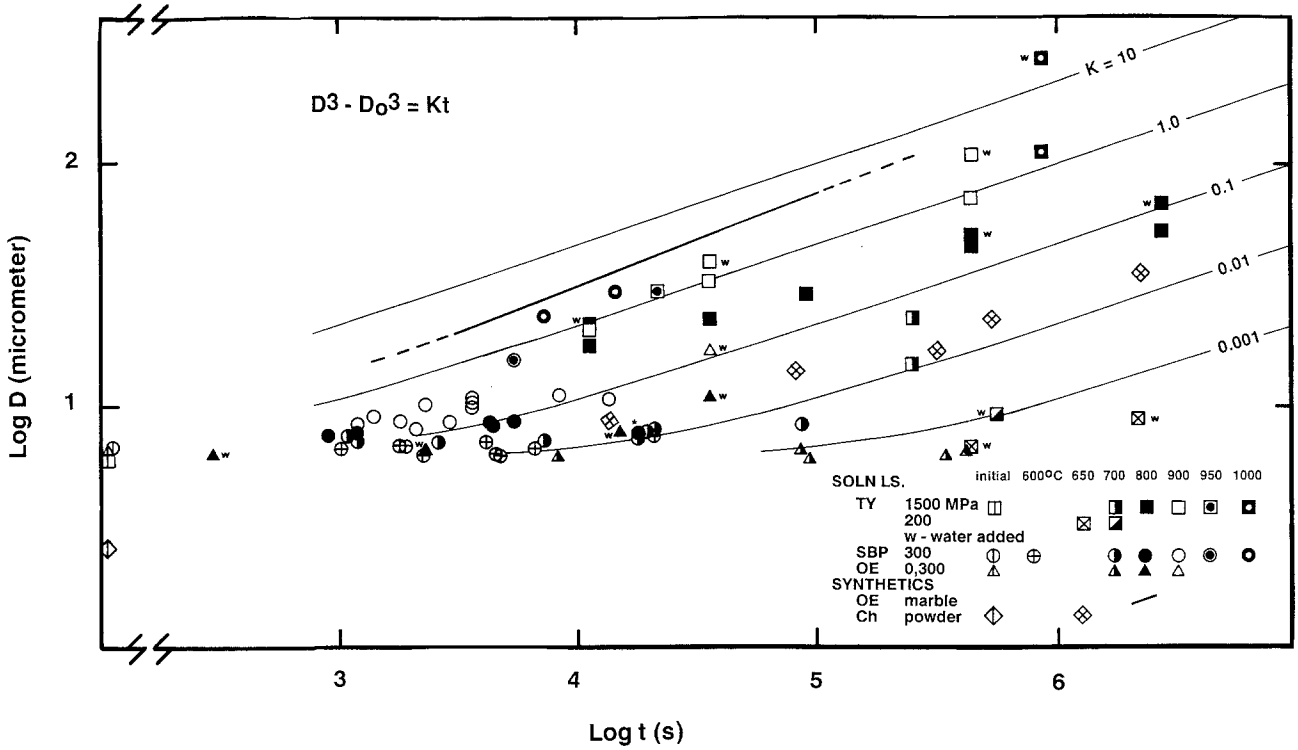

Fig. 10. Normal grain growth data for Solnhofen limestone at various temperatures and water contents from Tullis and Yund (1980) (TY); Schmid et al. (1977) and Schmid (private communication) (SBP); and the present study (OE). Also plotted are data for particle coarsening of $CaCO_3$ powders loosely packed in distilled water and heated to 650° C (Chai 1974) (Ch). Samples from Schmid et al.'s work (*circles*) which were heated, but not deformed, are marked with an *asterisk*. The diagram is contoured in orders of magnitude of K [see (1)] assuming $n=3$. *Solid line* is for the CA−XX data at 800° C

volume fractions of 600 and 2 ppm, respectively. Such volume fractions are less than that of even the purest marbles.

Thus, the existence of marbles with relatively large grain sizes implies that: 1) second phase particles in those marbles were larger than 5 μm, or were mobile and could coarsen as the matrix grain size increased, 2) grain growth was driven by additional internal energies, which were capable of overcoming the pinning forces. Very fine grain sizes imply: 1) the rocks were never exposed to high temperatures (>300° C) for even brief periods of time, 2) significant amounts of second phases are present, or 3) the grain size is in equilibrium with deviatoric stress.

Inhibition of normal grain growth by second phases

Mica particles in volume fractions of 1 and 5% were very effective at pinning grain boundaries and stabilizing the grain size (Fig. 8), results which are similar to experiments using Al_2O_3 as a second phase in synthetic marbles (Fig. 9). The value of the dispersion parameter, m, for marbles with added mica is 0.29, but is only a rough estimate because of the absence of data at other volume fractions, and the variations in porosity from sample to sample. For each of three long-term experiments (2005, 2007, 2053) that contained both 1 and 5 percent specimens, $m=0.35\pm0.03$.

Mica particles were more commonly distributed along grain boundaries and corners than in interiors, consistent with models where $m\approx0.3$–0.5 (Olgaard and Evans 1986). Mica plates along grain boundaries were aligned with their shortest axis normal to the boundary plane (Fig. 4c). At grain corners, the mica plates were more often randomly oriented in clusters and appeared to be suspended in a fluid (Fig. 4d). Such clustering was also observed for Al_2O_3 particles (Olgaard and Evans 1986). Although most of the clusters were probably the result of non-uniform initial dispersion, some "coarsening" would be expected if the particles were mobilized by the fluid boundary phase (Ashby and Centamore 1968) increasing the effective size and the fraction at grain corners with time. On boundaries the effective pinning size is the maximum plate dimension; at grain corners it is the diameter of the clusters. From microscope measurements, these diameters appeared to be 1–5 μm; substituting in (2), this suggests $C\sim1$, in agreement with theory (Fig. 9).

As discussed above, pores are also very effective at controlling the calcite grain size, and exert a drag force on the grain boundary that is proportional to their size and the number of pores which are intersected by the boundary. If the matrix material can be transported by diffusion or solution transport in a pore fluid, the pores may coarsen with time, and only slow the boundaries (rather than pin them). A relationship between D and the instantaneous value d/f should therefore be established. If either d increases, e.g. by coarsening, or f decreases, perhaps during lithification, D_{max} would increase accordingly.

These results are consistent with quantitative studies of metals and ceramics (see Olgaard and Evans 1986), qualitative results for ice (Wilson 1979), and observations in natural samples (Robinson 1971; Hobbs et al. 1976; Etheridge and Wilke 1979; Christie and Ord 1980; Evans et al. 1980; Lisle and Savage 1982). We suppose that (2) is generally applicable to many different second phases or matrix materials.

Comparison to other data

In Fig. 10, grain growth data for Solnhofen limestone (Tullis and Yund 1982; Schmid et al. 1977; Schmid unpubl. data; and this study), and coarsening data for reagent-grade $CaCO_3$ powder loosely packed in water (Chai 1974), are compared to (1) fit to the CA−XX data ($n=2.6$) (solid line). The experimental studies differ in several important aspects: a) Tullis and Yund (1982) heat-treated Solnhofen limestone specimens with and without added water in a solid medium apparatus ($P_c=1500$ MPa) or in an argon-confining medium apparatus (200 MPa) at 650–1000° C. b) Schmid et al. (1977) measured the grain size in oven-dried Solnhofen limestone heated to 600–1000° C in an argon confining medium apparatus at $P_c=300$ MPa. With one exception, the specimens were heat-treated and subsequently deformed at constant displacement rate in the superplastic regime at a lower temperature. c) Chai (1974) measured the coarsening of calcite grains suspended in various chloride solutions. Figure 10 shows only the results for distilled water. In Table 4, the results from the fastest (2.0 N $CaCl_2$) and slowest growth rates (distilled H_2O) are given. The initial calcite powder size was 2.5 μm.

In all cases, the run time is the elapsed time at maximum temperature, so that differences in heat-up and quench times are systematic errors. Linear intercept lengths have been converted to D as above.

Several general observations can be made from these four studies: Normal grain growth was 1) faster in the synthetic marble than in Solnhofen limestone in all apparatus at a given temperature; 2) more rapid in Solnhofen in the solid medium apparatus at 1500 MPa than in the gas apparatus at lower pressures; 3) significant at 700° C and 1500 MPa, but negligible below 800° C at 400 MPa or less; 4) faster with added water at high pressure (1500 MPa); 5) only slightly affected by the addition of water at lower pressures; 6) relatively unaffected by confining pressure in experiments at lower pressures in which no water was added, or in which the sample was oven-dried. Finally, at 650° C, hydrothermal grain coarsening (Chai 1974) was slower than normal grain growth in the synthetic marbles but faster than that in Solnhofen limestone.

Grain size changes in Solnhofen measured after deformation experiments (Schmid et al. 1977) are possibly influenced by dynamic recrystallization (Poirier and Guillopé 1979; Urai et al. 1986). Dynamic recrystallization during dislocation creep often reduces grain size, but increases in grain size are commonly observed during superplastic flow (Wilkinson and Cáceres 1984). Apparently deformation in the superplastic region does not markedly increase growth kinetics in Solnhofen.

The most important effect of both confining pressure and the addition of water may have been to include melting. Adding water to dry marble lowers the melting point from 1300° C to less than 700° C (Wyllie and Boettcher 1969). In grain growth experiments in calcite with added water, Olgaard and Evans (1986) detected grain boundary films of cryptocrystalline or amorphous material which probably resulted from a melt phase at temperatures of 700° C and above. Thus, when water was available, even in small amounts, melt phases may have existed along the boundaries in the Solnhofen experiments.

Increasing the pressure from 300 MPa to 1500 MPa lowers the melting point by approximately 50° C. If melt phases are present, and wet a significant fraction of the grain boundaries, they may mobilize second phase particles lying along grain boundaries. The question of melt in the Solnhofen experiments was not addressed, although at 950–1000° C, Schmid (private comm.) observed large bubbles that may have contained melt (Fig. 5d). The growth rate in those experiments was comparable to other experiments done at 1500 MPa even though Schmid's samples were oven-dried beforehand.

For the loosely packed calcite powders (Chai 1974), coarsening was probably controlled by mass transfer through the fluid phase. The kinetic equations for coarsening of particles suspended in a fluid are similar to normal growth of grains with a thin boundary fluid film (Lay 1968); the coarsening rate is predicted to vary inversely with the fluid film thickness. Thus, normal grain growth in synthetic marbles with fluids may be faster than in the loosely packed powders because the amount of fluid, i.e. film thickness, is smaller. The slower growth rates in Solnhofen limestone may be attributed to the influence of second phases in the limestone, or to differences between transport mechanisms which operate in the fluid coarsening), or along the grain boundaries (in the Solnhofen).

Table 4. Growth rate constants, K, and grain size exponent, n, for calcite grain growth

Calcite rock	T (° C)	P_c (MPa)	K[a] (10^{18} m^3/s)	n
Synthetic marbles				
1007–4003 P	900	400/300	7.0–13.0	4.2
1007–4003 P	800	400/300	0.2– 9.0	
1007–4003 P	700	400/300	0.1– 0.25	2.9±0.5
CA-2–15 P	800	300	2.4– 4.8	2.6±0.1
CA-2–15 P	650	500	0.2– 3.0	
CA-2–15 P	550	500	0.25	
Solnhofen limestone				
Tullis & Yund	1000 W	1500	22.0	
Tullis & Yund	900	1500	2.0– 3.0	2.5
Tullis & Yund	800	1500	0.1– 0.9	4.8
Tullis & Yund	700	1500	0.04	
Tullis & Yund	1000 D	1500	1.5	
Tullis & Yund	950	1500	1.1	
Tullis & Yund	900	1500	0.8 –1.0	3.0
Tullis & Yund	800	1500	0.05–0.5	5.1
Tullis & Yund	700	1500	0.05–0.6	
Tullis & Yund	700	200	0.001	
Tullis & Yund	650	200	0.0002	
Schmid et al.	1000	300	2.0	2.5
Schmid et al.	950	300	0.7	
Schmid et al.	900	300	0.08 –0.4	4.8
Schmid et al.	800	300	0.02 –0.2	>7
Schmid et al.	700	300	0.005–0.2	
Schmid et al.	600	300	0.007–0.09	
This study	900	300	0.1	
This study	800	300	0.03 –0.13	5.2
This study	700	0.1	<0.001	
Loosely packed powders				
Chai	distilled H_2O 650	200	0.015–0.13	3.7
	2.0 N $CaCl_2$ 650	200	0.9 –1.2	3.0

[a] Assuming $n=3$ and $D_0=7$ μm for synthetic marble, $D_0=6.1$ μm for Solnhofen limestone, and $D_0=2.5$ μm for the powders

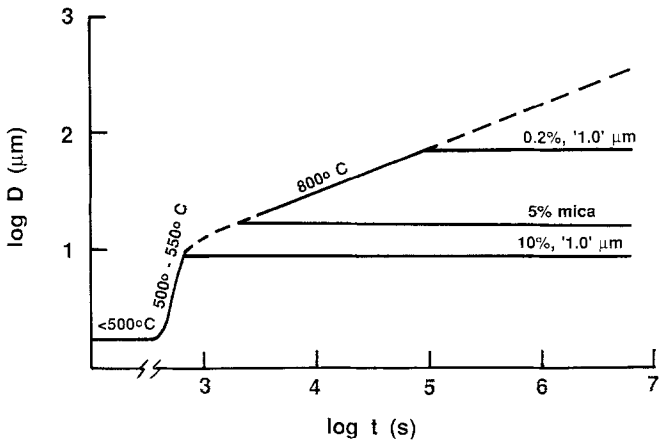

Fig. 11. Schematic summary of synthetic marble data. The highest densities were achieved when samples were fabricated at less than 500° C; primary recrystallization occurred between 500 and 550° C; normal grain growth began below 650° C and was relatively rapid at 800° C. The grain size was stabilized in a short time with even minor amounts of second phases. Numbers in single quotes (e.g. '1.0') are the nominal grit size in μm of the second phase Al_2O_3 particles added (Olgaard and Evans 1986). The stabilized grain sizes of samples containing mica agree with those containing Al_2O_3

Linear regressions of the grain growth data of Tullis and Yund (1980) and Schmid et al. (1976) for Solnhofen limestone, and the hydrothermal grain growth data of Chai (1974) for reagent grade powders, gave exponents ranging from 2.5 to greater than 4, with n tending to increase with decreasing temperature (Table 4).

Summary and conclusions

The evolution of grain size in these experiments is shown quantitatively in Fig. 11. Densification without recrystallization occurred within one hour at 500° C. Primary recrystallization of the densified material and the initial stages of normal grain growth occurred within 1–2 h at 500–550° C and resulted in increases in grain size by factors of 2 to 5. Normal grain growth occurred in the synthetic marble at all temperatures above 550° C. The grain growth data are described by (1) with n equal to 2.6. Grain sizes increased to 65 μm in 24 h at 800° C.

With the addition of pores, mica, or alumina, a stabilized grain size resulted. Once the stabilized size is reached, growth can continue only if the second phases are mobile, or if new driving forces are introduced which cause unpinning; e.g., deformation or phase transformations. Thus, at least two situations exist where grain size is independent of time and temperature, even at moderate to high temperatures: when the dynamically recrystallized grain size is a function of deviatoric stress, and when second phases pin the boundaries. In the latter case, grain size is a function of second-phase diameter, volume fraction, and dispersion.

Substantial variations in normal grain growth kinetics result from second phases, dissolved impurities, and pores; more detailed experiments are needed to determine the exact influence of each of those parameters on growth rates. In addition, once kinetic laws are determined, to apply them to geologic situations will require careful characterization of the composition and texture of the natural materials. One important step in understanding the grain size history involves determining matrix and second phase size distributions, as well as second phase volume fractions. Finally, the calcite/mica and calcite/alumina data show systematics which are very similar to normal grain growth in ceramics and metals; thus, it is also likely that similar second phase effects will occur during normal grain growth of other minerals including olivine, feldspar, quartz, halite or ice.

Acknowledgments. We thank S. Schmid (ETH) for useful discussions, some unpublished data, and reviewing the manuscript. We gratefully acknowledge NSF for financial support (EAR-8108560 and EAR-8520643) and ARO for an equipment grant (DAAG29-85-G-0011). The Swiss National Science Foundation supported D.L. Olgaard while the manuscript was completed.

References

Allen T (1981) Particle size measurement. Chapman and Hall, London

Anand L, Gurland J (1975) The relationship between the size of cementite particles and the subgrain size in quenched-and-tempered steels. Metall Trans A 6A:928–931

Anderson MP, Srolovitz DJ, Grest GS, Sahni PS (1984) Computer simulation of grain growth – I. Kinetics. Acta Metall 32:783–791

Anderson TF (1969) Self-diffusion of carbon and oxygen in calcite by isotope exchange with carbon dioxide. J Geophys Res 74:3918–3932

Ashby MF (1980) The influence of particles on boundary mobility. In: Hansen N, Jones AR, Leffers T (eds) Recrystallization and grain growth of multi-phase and particle containing materials. Proc 1st Risø Int Symp Metall Mater Sci, pp 325–336

Ashby MF, Centamore RMA (1968) The dragging of small oxide particles by migrating grain boundaries in copper. Acta Metall 16:1081–1092

Barber DJ, Wenk HR (1973) The microstructure of experimentally deformed limestones. J Mater Sci 8:500–508

Barber DJ, Wenk HR (1979) On geological aspects of calcite microstructure. Tectonophysics 54:45–60

Bennison SJ, Harmer MP (1985) Grain-growth kinetics for alumina in the absence of a liquid phase. J Am Ceram Soc 66:C-22-C-24

Bernabé Y, Brace WF, Evans B (1982) Permeability, porosity and pore geometry of hot-pressed calcite. Mech Mater 1:173–183

Brook RJ (1976) Controlled grain growth. In: Wang FFY (ed) Treatise Mater Sci Technol, vol 9. Academic Press, New York, pp 331–364

Buerger MJ (1930) Translation-gliding in crystals. Am Mineral 15:45–64

Buerger MJ, Washken E (1947) Metamorphism of minerals. Am Mineral 32:296–308

Burke JE, Turnbull D (1952) Recrystallization and grain growth. Prog Met Phys 3:220–292

Caristan Y, Harpin RJ, Evans B (1981) Deformation of porous aggregates of calcite and quartz using the isostatic hot-pressing technique. Tectonophysics 78:629–650

Chai BHT (1974) Mass transfer of calcite during hydrothermal recrystallization. In: Hofmann AW, Giletti BJ, Yoder HS Jr, Yund RA (eds) Geochem Transp Kinet. Carnegie Inst, Washington, pp 205–218

Christie JM, Ord A (1980) Flow stress from microstructures of mylonites: example and current assessment. J Geophys Res 85:6253–6262

Drury MR, Humphreys FJ, White SH (1985) Large strain deformation studies using polycrystalline magnesium as a rock analogue. Part II: dynamic recrystallization mechanisms at high temperatures. Phys Earth Planet Int 40:208–222

Edwards AB, Baker G (1944) Contact phenomena in the Morang Hills, Victoria. Proc R Soc Victoria 56:19–34

Etheridge MA, Wilke JC (1979) Grain size reduction grain boundary sliding and the flow strength of mylonites. Tectonophysics 58:159–178

Evans B, Rowan M, Brace WF (1980) Grain-size sensitive deformation of a stretched conglomerate from Plymouth, Vermont. J Struct Geol 2:411–424
Exner HE (1972) Analysis of grain- and particle-size distributions in metallic materials. Int Metall Rev 17:25–42
Gladman T (1966) On the theory of the effect of precipitate particles on grain growth in metals. Proc R Soc London 294A:298–309
Goetze C, Kohlstedt DL (1977) The dislocation structure of experimentally deformed marble. Contrib Mineral Petrol 59:293–306
Greenwood GW (1956) The growth of dispersed precipitates in solutions. Acta Metall 4:243–248
Grest GS, Srolovitz DJ, Anderson MP (1985) Computer simulation of grain growth – IV. Anisotropic grain boundary energies. Acta Metall 33:509–520
Griggs DT, Paterson MS, Heard HC, Turner FJ (1960) Annealing recrystallization in calcite crystals and aggregates. Mem – Geol Soc Am 79:21–37
Grigor'ev DP (1965) Ontogeny of minerals. Isr Prog Sci Transl Jerusalem
Haroun NA, Budworth DW (1968) Modifications to the Zener formula for limitation of grain size. J Mater Sci 3:326–328
Hay RS (1987) Chemically induced grain broundary migration and thermal grooving of calcite bicrystals. Ph D Thesis, Princeton Univ, Princeton, New Jersey
Hellmann P, Hillert M (1975) On the effect of second-phase particles on grain growth. Scand J Metall 4:211–219
Herdan G (1960) Small particle statistics. Butterworths, London
Hobbs BE (1968) Recrystallization of single crystals of quartz. Tectonophysics 6:353–401
Hobbs BE, Means WD, Williams PF (1976) An Outline of Structural Geology. Wiley, New York
Hu H, Rath BB (1970) On the time exponent in isothermal grain growth. Metall Trans 1:3181–3184
Hsueh CH, Evans AG, Coble RL (1982) Microstructure development during final/intermediate stage sintering – I. Pore/grain boundary separation. Acta Metall 30:1269–1279
Janczuk B, Chibowski E, Staszczuk P (1983) Determination of surface free energy components of marble. J Colloid Interface Sci 96:1–6
Joesten R (1983) Grain growth and grain-boundary diffusion in quartz from the Christmas Mountains (Texas) contact aureole. Am J Sci 283-A:233–254
Jurewicz SR, Watson EB (1985) The distribution of partial melt in a granitic system: The application of liquid phase sintering theory. Geochim Cosmochim Acta 49:1109–1121
Keller WD, Viele GW, Johnson CH (1977) Texture of Arkansas novaculite indicates thermally induced metamorphism. J Sediment Petrol 47:834–843
Kingery WD, Bowen HK, Uhlmann DR (1976) Introduction to ceramics. 2nd ed. Wiley, New York
Kingery WD, Francois B (1965) Grain growth in porous compacts. J Am Ceram Soc 48:546–547
Kronenberg AK, Yund RA, Giletti BJ (1984) Carbon and oxygen diffusion in calcite: effects of Mn content and P_{H2O}. Phys Chem Miner 11:101–112
Lay KW (1968) Grain growth in $UO_2-Al_2O_3$ in the presence of a liquid phase. J Am Ceram Soc 51:373–376
Lifshitz IM, Slyozov VV (1961) The kinetics and precipitation from superheated solid solutions. J Phys Chem Solids 19:35–50
Lisle RJ, Savage JF (1982) Factors influencing rock competence: Data from a Swedish deformed conglomerate. Geol Fören Stockholm Förh 104, Pt. 3:219–224
Louat N (1983) The inhibition of grain-boundary motion by a dispersion of particles. Philos Mag A 47:903–912
Nes E, Ryum N, Hunderi O (1985) On the Zener drag. Acta Metall 33:11–22
Nichols FA (1966) Theory of grain growth in porous compacts. J Appl Phys 37:4599–4602
Nielsen JP (1966) Some laws of grain growth. In: Recrystallization, grain growth and textures. ASM, Metals Park, Ohio, pp 286–294
Olgaard DL (1985) Grain growth and mechanical processes in two-phased synthetic marbles and natural fault gouge. PhD Thesis, Massachusetts Institute of Technology, Cambridge, Massachusetts
Olgaard DL, Evans B (1986) Effect of second-phase particles on grain growth in calcite. J Am Ceram Soc 69:C-272–C-277
Poirier J-P, Guillopé M (1979) Deformation induced recrystallization of minerals. Bull Mineral 102:67–74
Robinson D (1971) The inhibiting effect of organic carbon on contact metamorphic recrystallization of limestones. Contrib Mineral Petrol 32:245–250
Rosenholtz JL, Smith DT (1949) Linear thermal expansion of calcite, var. Iceland spar and Yule marble. Am Mineral 34:846–854
Rossi G, Burke JE (1973) Influence of additives on the microstructure of sintered Al_2O_3. J Am Ceram Soc 56:654–659
Rutter EH (1983) Experimental static recrystallization and grain growth of calcite. J Geol Soc London 140:161
Schmid SM, Boland JN, Paterson MS (1977) Superplastic flow in fine grained limestone. Tectonophysics 43:257–291
Shewmon PG (1969) Transformations in metals. McGraw-Hill, New York
Skinner BJ (1966) Thermal expansion. In: Clark SP Jr (ed) Handbook of physical constants. Mem Geol Soc Am 97:75–96
Smith CS (1948) Grains, phases and interfaces: an interpretation of microstructure. Trans AIME 175:15–51
Spry A (1969) Metamorphic Textures, Pergamon Press, Oxford
Srolovitz DJ, Anderson MP, Grest GS, Sahni PS (1984) Computer simulation of grain growth – III. Influence of a particle dispersion. Acta Metall 32:1429–1438
Takeuchi S, Argon AS (1976) Review: Steady-state creep of single-phase crystalline matter at high temperature. J Mater Sci 11:1542–1566
Tullis J, Yund RA (1982) Grain growth kinetics of quartz and calcite aggregates. J Geol 90:301–318
Underwood EE (1970) Quantitative stereology. Addison-Wesley, Reading, Mass
Urai JL, Means WD, Lister GS (1986) Dynamic recrystallization of minerals. In: Mineral and Rock Deformation: Laboratory Studies – The Paterson Volume. Geophys Monogr Am Geophys Union 36:161–199
Wagner C (1961) Theorie der Alterung von Niederschlègen durch Umlösen, (Ostwald-Reifung). Z Elektrochem 65:581–591
Wilkinson DS, Cáceres CH (1984) An evaluation of available data for strain-enhanced grain growth during superplastic flow. J Mater Sci Lett 3:395–399
Wilson CJL (1979) Boundary structures and grain shape in deformed multi-layered polycrystalline ice. Tectonophysics 57:T19–T25
Wong T-F, Brace WF (1979) Thermal expansion of rocks: some measurements at high pressure. Tectonophysics 57:95–117
Wyllie PJ, Boettcher AL (1969) Liquidus phase relationships in the system $CaO-CO_2-H_2O$ to 40 kilobars pressure with petrological applications. Am J Sci 267-A:489–508
Yan MF, Cannon RM, Bowen HK (1977) Grain boundary migration in ceramics. In: Fulrath RM, Pask JA (eds) Cermaic microstructures-76. Westview Press, Boulder, Colo, pp 276–307
Zener C (1948) Private communication to Smith CS, Grains, phases and interfaces: an interpretation of microstructure. Trans AIME 175:15–51

Received September, 1987 / Accepted July 1988
Editorial responsibility: V. Trommsdorff